

OPTIMAL DESIGN OF A PHOTOVOLTAIC STATION USING MARKOV AND ENERGY PRICE MODELLING

Marcio B. Salazar Márquez^{**,*}, Aouss Gabash^{*}, Yuri A. W. Shardt^{*}, Julio C. Tafur^{**}

^{*}TU Ilmenau University of Technology, Department of Automation Engineering, Germany

^{**}Pontifical Catholic University of Peru (PUCP), Department of Engineering, Peru

ABSTRACT

This paper addresses the optimization of photovoltaic (PV) systems to increase their efficiency. The study introduces a new pricing model that considers the current price of PV inverters. In addition, Markov modeling is used in a new optimization framework to determine the optimal configuration, considering the number of PV modules and inverters, operational constraints, and failure events of PV inverters up to 100 kW. A case study with six real PV inverters confirms the effectiveness of the proposed framework. It calculates the average daily hours of rated power generation considering geographic location, temperature, and solar irradiance using real data from a real PV system. The study identifies both local and global optimal solutions for PV inverters (15 kW to 100 kW), while minimizing the effective levelized cost of energy. The results of the study have important implications for future assessments of PV module failures and repairs.

Index Terms - Effective levelized cost of energy, price modelling, Markov modelling, optimal design, photovoltaic (PV) inverters, PV station

1. INTRODUCTION

Renewable energy systems, particularly photovoltaic (PV) technology, are gaining traction as a viable solution to address increasing energy demand [1]–[5]. Governments promote PV station investments to address pollution and reduce reliance on traditional fuels, for example, solar energy in the United States is expected to triple within a span of five years [6]. A PV station or plant comprises PV panels that generate direct current (DC) and PV inverters that convert DC to alternating current (AC) [7]. Hence, the optimal design of PV stations, which has a significant effect on efficiency, investment cost, and power generation reliability, becomes crucial in meeting the increasing demand for renewable energy systems [8]. There are four groups in which PV stations can be classified based on the arrangement of PV modules, inverters, and interconnection methods: centralized, string, multistring, and AC modular configurations [9]. Note that the classification of PV stations into different groups based on their arrangement and configuration can impact the cost of energy.

The levelized cost of energy (LCOE) [8], [9] is a metric used to estimate the average cost of electricity generated by a power plant over its lifetime. It takes into account the initial investment, operational and maintenance costs, fuel costs, and expected energy production. LCOE is commonly used to compare the economic viability of different energy sources or power generation technology. On the other hand, the effective levelized cost of energy (ELCOE) goes beyond the traditional LCOE by incorporating the economic availability of the power plant. ELCOE takes into consideration factors such as downtime, maintenance, and other



operational constraints that affect the actual energy output of the plant. By considering these factors, ELCOE provides a more accurate representation of the economic performance and feasibility of a power plant or system.

Markov modelling [9], [10] is a mathematical technique that analyses and predicts the behaviour of systems undergoing a series of discrete events. It uses Markov chains, mathematical models representing systems transitioning between different states over time. Assuming that the system's future behaviour solely depends on its current state, that is, if obeys the Markov assumption, probabilistic models can be constructed to describe state transitions. Markov modelling enables the analysis of complex systems with uncertain behaviours, facilitating predictions and decision optimization. In renewable energy systems, Markov modelling assesses reliability, performance, and maintenance needs of components like PV inverters by analysing failure and repair probabilities through state transitions using a stochastic transitional probability matrix [11], optimizing their operation and design.

Not supplied expected energy (NSEE) [9] is a metric that evaluates the availability of a power generation system, specifically renewable energy sources like PV systems. It measures the energy that the system fails to deliver due to factors such as downtime, equipment failures, and maintenance. NSEE considers plant size, weather conditions, and component performance, providing insights into system reliability. It helps assess the economic impact of energy losses and enables optimization of system efficiency and availability.

This work introduces a new optimal design method that is being developed for a real PV station with an installed peak power of 86 kW_p, using Markov and energy price modelling. The data of injected energy from the station is available, comprising four samples per hour for one year (35,040 samples). The key contributions are:

- A new method is developed to determine the power generation of PV stations over a year, considering geographical location, temperature, and the number of sunny days in Germany.
- A new pricing model is created that takes into account the current prices for PV inverters in 2022.
- An optimization framework combining Markov modelling and the new pricing model is proposed to achieve the optimal design of a PV station.
- Real data for six different sizes of PV inverters are used in the design process, and the results obtained are compared with previous studies to demonstrate the effect of the new price modelling approach.

2. MODELLING OF A PHOTOVOLTAIC STATION

PV stations consist of two main components: (1) PV panels, which are composed of PV modules, and (2) PV inverters. In a PV station installation, the voltage of a PV panel array can range from 300 to 1000 V, with currents varying from 5 to 10 A [7]. PV inverters play a crucial role in converting the DC power generated by PV panels into AC power. In grid-connected PV stations, the inverters are designed to operate in parallel with the electrical utility grid systems. The PV modules supply DC power, which is directly connected to the inverters. The inverters produce AC power that can be used by the load or fed into the grid system synchronously in case of excess power. The AC power output is directly proportional to the photovoltaic DC source [7]. Figure 1 shows the block diagram of a general PV station [8].

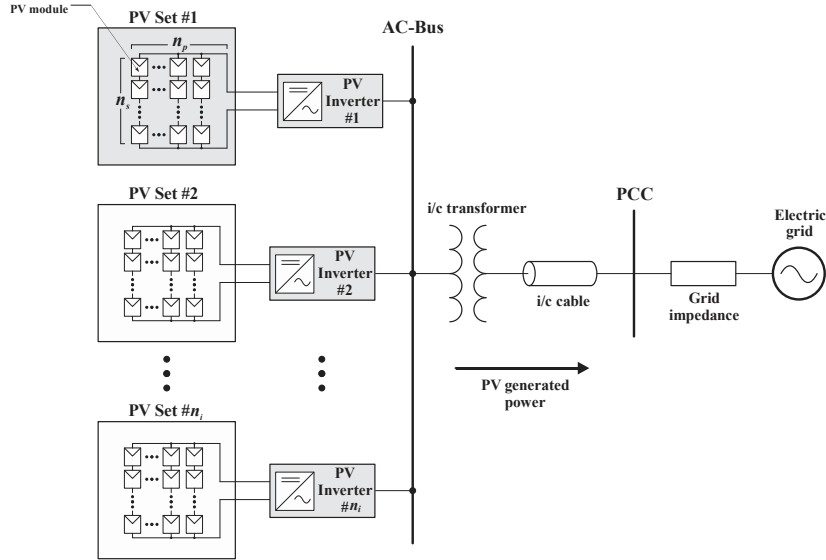


Figure 1: Generalized block diagram of a PV station [8].

Multiple PV inverters are used to establish the connection between the DC output voltage of PV modules and the AC power grid. The total number of PV modules is determined by the size, characteristics, and the maximum capacity permitted by the PV station, considering the total number (n_i) of PV inverters. A PV set, consisting of an array of PV panels, is formed by connecting a specific number (n_p) of PV parallel panels. Each PV panel comprises a specific number (n_s) of PV series modules. Each DC/AC PV inverter is connected to the DC input of a PV set and is equipped with an integrated maximum power point tracking system to optimize power extraction. Surge protection devices are integrated into the inverters to safeguard the PV system against lightning strikes, managing transient overvoltage and current redirection [12]. The AC output power from the PV inverter is injected into the electric grid at the point of common coupling (PCC), as shown in Figure 1. Interconnecting (i/c) transformers and cables facilitate the transmission of AC power from the inverter to the grid.

3. PROPOSED OPTIMAL DESIGN

To ensure a reliable design of a PV station, it is essential to estimate the energy not supplied within the system [9]. This estimation is influenced by factors such as the total number of PV panels and inverters, their interconnections, and the reliability characteristics of individual components. Two key parameters for reliability assessment are introduced [11]: (1) the mean time between failures (MTBF), calculated as the total operating time divided by the total number of failures, and (2) the mean time to repair (MTTR), calculated by dividing the total repair time by the number of repairs or by using the average repair time for a specific component or system. In general, the failure rate (λ) and repair rate (μ) in systems can be calculated using various methods depending on the available data and the nature of the system. In this paper, these rates are calculated as [9]

$$\lambda = \frac{1}{\text{MTBF}} = \lambda_b \times \pi_A \times \pi_E \times \pi_Q \times \pi_T \left[\frac{\text{Failures}}{1\text{-year}} \right] \quad (1)$$

$$\mu = \frac{1}{\text{MTTR}} = \frac{1}{T_d} \left[\frac{\text{Repairs}}{1\text{-year}} \right] \quad (2)$$

where λ_b is the base failure rate, π_A the application factor, π_E the operation environment factor, π_Q the quality factor, π_T the temperature factor. The term $T_d = \text{MTTR}$ corresponds to the time in days required to repair a PV inverter. In PV stations, component failure and repair rates are typically considered constant, assuming random failures distributed uniformly over the station's lifetime. Studies and field research indicate that failures mainly occur in power electronic interfaces within the PV station [13]. The system's reliability is primarily affected by the number of PV inverters and their interconnection structure.

The conventional LCOE, as mentioned earlier, is a measure of the cost per unit of energy consumed, usually expressed in US dollars per kilowatt-hour (\$/kWh). It considers various costs, such as capital costs and operating costs. In contrast, the ELCOE, introduced in [9], is an enhanced version of LCOE that additionally incorporates maintenance, repair, and replacement costs of PV inverters over the lifetime of the PV station. The costs, including maintenance, repair, and replacement costs of PV inverters over the PV station's lifetime, are estimated using probabilities and state transitions derived from Markov modelling, as explained in the next section, while the ELCOE can be calculated as [9]

$$\text{ELCOE} = \frac{\text{Total effective cost}}{\text{Total effective generated energy}} \text{ [$/kWh]} \quad (3)$$

3.1 Markov Modelling

Markov modelling is a widely used technique for analysing solar-powered systems characterized by stochastic models. The stochastic nature of these systems presents a significant challenge in developing reliable algorithms, methods, and tools for their analysis and quantification. Note that the future states in a Markov model depend solely on the current state, independent of previous states [11]. Figure 2 shows the Markov model for a PV station with multiple states denoting the number of PV inverters.

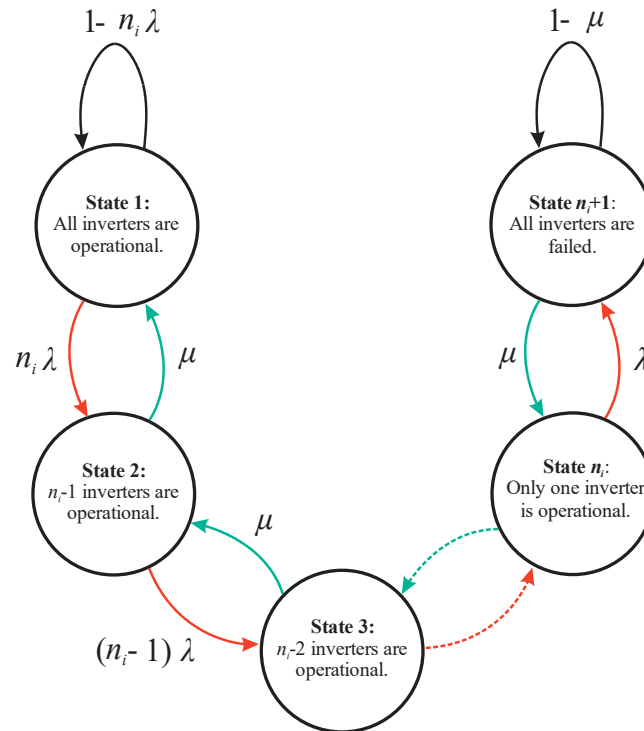


Figure 2: States and transitions of a PV station in the Markov model [9].

In state 1, all n_i inverters are operational, and transitions to subsequent states occur due to failure probabilities. For instance, in state 2, $(n_i - 1)$ inverters remain operational. Upon experiencing a failure event indicated by the red arrow, an inverter fails and progresses to the next state. This process continues until all inverters fail, reaching the final state $(n_i + 1)$. Repair probabilities, represented by green arrows, allow inverters to return to the previous state. The Markov model facilitates the calculation of the stochastic transitional probability matrix A as [9]

$$A = \begin{bmatrix} 1 - n_i \lambda & n_i \lambda & 0 & 0 & \cdots & 0 \\ \mu & 1 - \mu - (n_i - 1) \lambda & (n_i - 1) \lambda & 0 & \cdots & 0 \\ 0 & \mu & 1 - \mu - (n_i - 2) \lambda & (n_i - 2) \lambda & \cdots & 0 \\ 0 & 0 & \mu & 1 - \mu - (n_i - 3) \lambda & \cdots & \vdots \\ \vdots & \vdots & \vdots & \vdots & \vdots & \lambda \\ 0 & 0 & 0 & 0 & \mu & 1 - \mu \end{bmatrix} \quad (4)$$

where A represents the probabilities of transitioning between different states in a Markov model. Each element of the matrix corresponds to the probability of transitioning from one state to another. Specifically, the off-diagonal elements of matrix A , denoted as a_{ij} , represent the transition probabilities from state i to state j . The diagonal elements, denoted as $a_{ii} = 1 - b_i$, where b_i represents the sum of the exit transitions from state i . For example, the first element of matrix A , that is, $a_{11} = 1 - n_i \lambda$, represents the probability of transitioning to the same state 1. Similarly, the last element of matrix A , that is, $a_{n_i+1, n_i+1} = 1 - \mu$, where n_i+1 is the total number of states, represents the probability of transitioning to the same final state n_i+1 .

Moreover, the operating probabilities of the PV station are determined to estimate the system availability. The method for calculating these probabilities is described in [11] and [9]. According to this method, if p_k represents the probability of being in state k , the state probability vector P can be obtained as

$$P = PA \quad (5)$$

where

$$P = [p_1 \quad p_2 \quad p_3 \quad p_4 \quad \cdots \quad p_{n_i} \quad p_{n_i+1}] \quad (6)$$

To calculate the probabilities matrix from A , verify that each row of A sums up to 1, create a $1 \times n_i+1$ matrix P initialized with zeros and start in state 1, iterate over each entry in A and assign its value to the corresponding entry in P , resulting in P representing the probabilities of transitioning between the states.

For instance, Figure 3 shows the transient behaviour of a two-state system (left), that is, $n_i = 1$, and a five-state system (right), that is, $n_i = 4$, displaying the time-dependent values of the state probabilities.

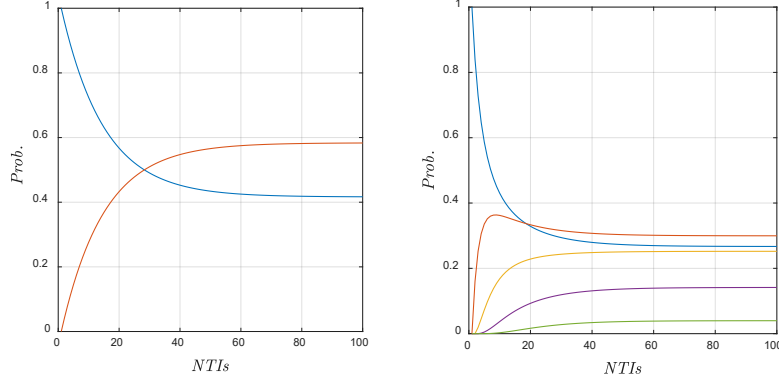


Figure 3: The transient behaviour of a two-state system (left) and a five-state system (right).

As the number of time intervals ($NTIs$) increases, the state probability values tend to converge to a constant value, indicating the system's adherence to the conditions of the Markov model. This steady state, representing the time-independent state probabilities, is observed on the y -axis. In the example of the two-state system, it is assumed that the system started in state 1, that is, one inverter which is operational, and the transient behaviour was evaluated as time increased, as shown in Figure 3(left). Note that the transient behaviour is highly influenced by the initial conditions [11]. Similarly, the transient behaviour of a five-state system is shown in Figure 3(right).

3.2 Price Modelling

The cost of a PV inverter was estimated in 2012 as

$$C_1(x) = \alpha_1 + \alpha_2 x - \alpha_3 x^2 + \alpha_4 x^3 \quad (7)$$

where x is the inverter size in kW, $C_1(x)$ is the cost in US dollars (USD) (\$), $\alpha_1 = 660$, $\alpha_2 = 480$, $\alpha_3 = 0.55$, and $\alpha_4 = 0.0005$ [9]. Note that this calculation does not account for price changes or inflation over time. To develop a new price model for PV inverters up to $x_{\max} = 100$ kW [14], the current price trend for commercial PV inverters and the above formula are used to estimate the cost of a PV inverter in 2022 as

$$C_2(x) = C_1(x) - \left(\frac{c_1 \times x}{c_2} \right) \quad (8)$$

where two factors are considered, that is, the first factor $c_1 = C_{1\text{kW}.2012} - C_{1\text{kW}.2022}$ which represents the difference between prices per kW in 2022 and 2012, while the second factor c_2 is assumed to be 3, accounting for the decline in component prices and the increase in efficiency. Figure 4 shows the flow diagram of the new price model. Note that the initial price for a 1-kW PV inverter is set at $C_{\text{init}.2022} = \$600$ for cost estimation purposes, when $x = 1$ kW, corresponding to the centralized topology. Furthermore, the cost of inverters in 2022 is also taken into account, where $C_{1\text{kW}.2012} = \$1140$ [9], $C_{1\text{kW}.2022} = C_{1\text{kW}.2012} / c_0$, and c_0 is assumed to be 4 given lower prices. Figure 5 shows the trend of inverter costs relative to their size, indicating significant changes in prices over the past 10 years based on current commercial data. The proposed new price model assumes that the cost of a 1-kW inverter in 2022 is lower than in 2012.

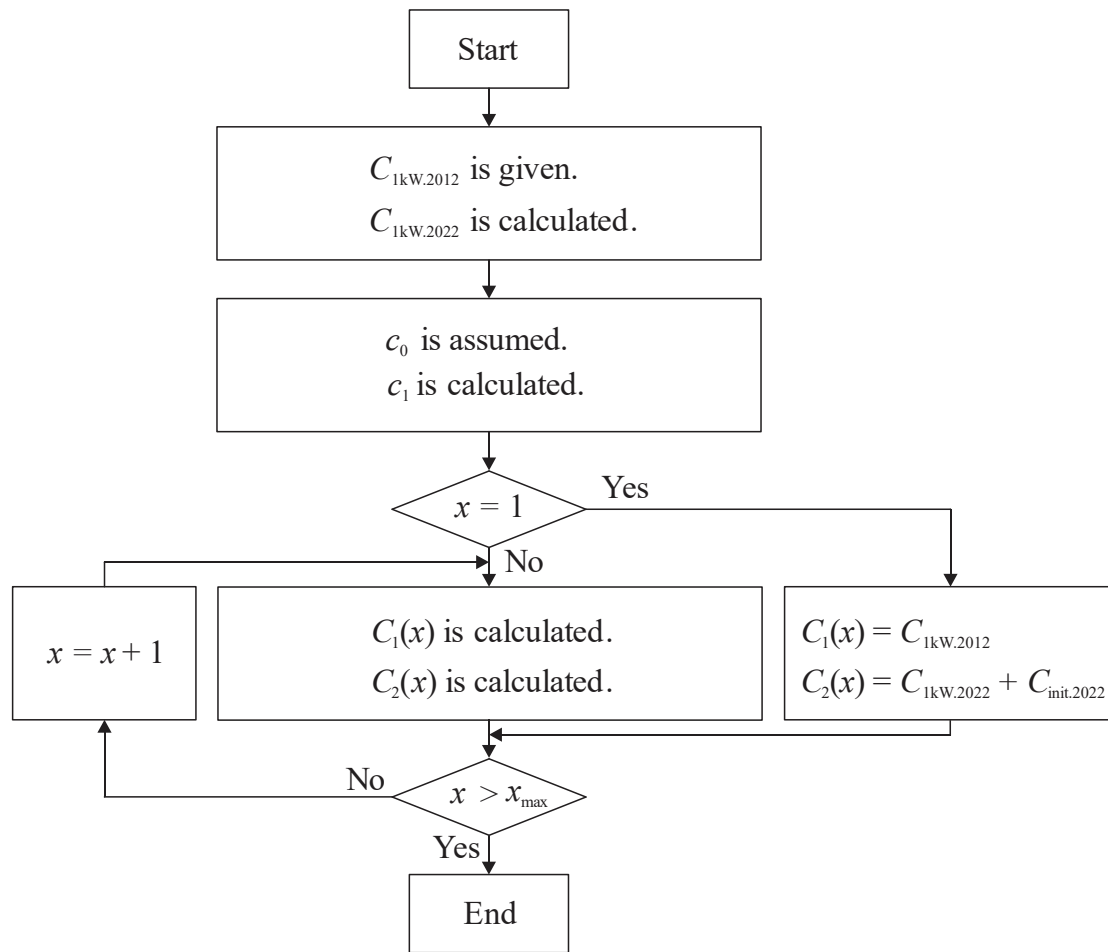


Figure 4: Flow diagram of the new price model.

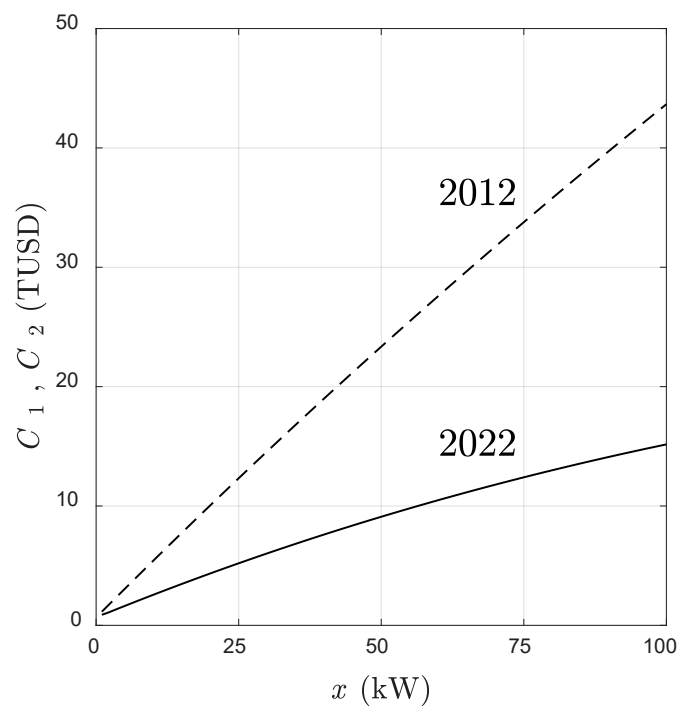


Figure 5: PV inverter cost in 2012 and 2022 versus inverter size.

3.3 Geographical Conditions

The proposed optimal design is applicable to PV stations with a capacity of up to 100 kW considering real geographical conditions. Hence, real data of injected energy is obtained from a reference PV station situated in Langewiesen, Germany. The data were provided free of charge by Thüringer Energienetze GmbH [15], [16]. The following data features are extracted from the available information: (1) the installed peak power of the PV panels $P_{tot} = 86$ kilowatt-peak (kWp), (2) there are four samples per hour over the course of one year, resulting in a total of 35,040 samples, (3) the actual annual energy generated by the PV modules $E_{real} = 73,713$ kWh, (4) the ideal annual energy generation by the PV modules $E_{ideal} = 749,295$ kWh, and (5) the maximum power generated reaches 68 kW. Note that kWp is a unit for measuring the power of photovoltaic systems, enabling comparison between modules, and it is calculated by multiplying the power of one module by the number of installed modules [17].

The average daily hours during which a PV module operates at its rated power is defined as [9]

$$h = \frac{TGEY}{365 \times P_{tot}} \quad (9)$$

where $TGEY$ is the total generated energy in kWh over the course of a year. However, in [9], the value of h is assumed to be 6 [hours/day] based on the geographical location. In this paper, we calculate $TGEY$ based on the available data as follows

$$TGEY = IGEY \times PV_{factor} \quad (10)$$

where $IGEY$ denotes the ideal amount of generated energy in kWh per year, calculated as

$$IGEY = P_{tot} \times N_D \times N_H \quad (11)$$

where $N_D = 365$ is the number of days per year, $N_H = 24$ is the number of hours per day, and PV_{factor} is defined as

$$PV_{factor} = \frac{E_{real}}{E_{ideal}} \quad (12)$$

Using the available data, we get $PV_{factor} = 0.098 \approx 0.1$, that is, 10 [%]. This yields a value of hours per day

$$\begin{aligned} h &= \frac{IGEY \text{ [kWh]} \times PV_{factor} \text{ [%]}}{365 \text{ [day]} \times P_{tot} \text{ [kW}_p\text{]}} \\ &= \frac{753,360 \text{ [kWh]} \times 10 \text{ [%]}}{365 \text{ [day]} \times 86 \text{ [kW}_p\text{]}} = 2.4 \text{ [hours/day]} \end{aligned}$$

which is lower than the value given in [9].

3.4 Not Supplied Expected Energy

Based on the information provided, an essential factor for the optimal design is the calculation of the not supplied expected energy associated at state k ($NSEE_k$), in which $k - 1$ inverter are out of service. This factor represents the energy that is expected to remain unsupplied by the system due to component failures or other operational factors. The value of $NSEE_k$ can be calculated as [9]

$$NSEE_k = (k - 1) \times x \times h \times T_d \quad (13)$$

while the metric NSEE can be calculated as

$$NSEE = \sum_{k=1}^{n_i+1} p_k NSEE_k = \sum_{k=1}^{n_i+1} p_k (k - 1) \times x \times h \times T_d \quad (14)$$

3.5 PV Station Configuration

The required number of inverters n_i is [9]

$$n_i(x) = \left\lceil \frac{P_{tot}}{x} \right\rceil \quad (15)$$

while the minimum number of modules connected in series ($n_{s,min}$) in each PV string can be calculated using the commercial technical data of the PV modules and inverters [8]

$$n_{s,min} = \min \left[\left\lceil \frac{V_{i,max}}{V_{PV}} \right\rceil, \left\lfloor \frac{V_{DC,max}}{V_{oc,max}} \right\rfloor \right] \quad (16)$$

where $V_{i,max}$ represents the PV inverter DC input maximum power point voltage, V_{PV} denotes the rated voltage of PV panels, $V_{DC,max}$ indicates the PV inverter maximum permissible DC input voltage, and $V_{oc,max}$ represents the PV module maximum open-circuit voltage. Finally, the number of inverters connected in series n_s and in parallel n_p can be calculated as

$$n_s = \left\lceil \frac{V_x}{V_{PV}} \right\rceil \quad (17)$$

$$n_p = \left\lfloor \frac{\frac{P_{tot}}{n_i}}{\frac{n_{s,min}}{P_{PV}}} \right\rfloor \quad (18)$$

where V_x represents the DC-side voltage of the PV inverter and P_{PV} represents the rated power of a PV module. The ceil function $\lceil \cdot \rceil$ rounds up to the nearest integer, while the floor function $\lfloor \cdot \rfloor$ rounds down to the nearest integer.

3.6 Effective Levelized Cost of Energy

The final design step is the calculation of the ELCOE as

$$\text{ELCOE} = \frac{C_{t(inv)}}{E_{y(eff)}} \quad (19)$$

where $C_{t(inv)}$ represents the total inverter cost during the lifetime of the PV station and $E_{y(eff)}$ represents the amount of effective generated energy in a year [9]. The numerator $C_{t(inv)}$ is defined as

$$C_{t(inv)} = C_{i(inv)} + C_{r(inv)} \times N \quad (20)$$

where N is the lifetime of the PV station in years, $C_{i(inv)}$ is the initial investment costs, and $C_{r(inv)}$ represents the estimation of repair or replacement costs of inverters in a year, which can be calculated as

$$C_{r(inv)} = \sum_{k=1}^{n_i+1} p_k \times ((k-1) \times rr + w \times TD_k) \quad (21)$$

where $TD_k = (k-1) \times \text{MTTR}$ is the downtime of the faulty PV inverters, w is the wage for skilled workers during the downtime, and rr is the repair costs of the inverters, which depends on their size [9]. The denominator $E_{y(eff)}$ is defined as

$$E_{y(eff)} = \sum_{k=1}^{n_i+1} p_k \times \eta \times h \times (n_i + 1 - k) \times (365 - T_d) \times x \quad (22)$$

where η is the efficiency of the PV station [9]. The design algorithm, as shown in Figure 6, outlines the design process, with inputs including the average energy production time of the panels h and the cost functions $C_1(x)$ and $C_2(x)$.

4. RESULTS

Six different sizes of PV inverters were used to assess and identify the optimal design for a PV station, including 100 kW ($n_i = 1$), 50 kW ($n_i = 2$), 30 kW ($n_i = 3$), 25 kW ($n_i = 4$), 20 kW ($n_i = 5$), and 15 kW ($n_i = 6$). The design results are presented in Table 1. It can be observed that as the inverter size increases, the failure rate of PV inverters tends to increase, while the repair rate decreases. In addition, the NSEE increases when a lower number of inverters are employed. This is attributed to higher failure probabilities associated with a reduced number of transition states in the reliability assessment conducted using the Markov model.

The results are shown in Figure 7, where in Figure 7(a), it can be observed that larger inverter sizes correspond to higher amounts of energy not supplied. The NSEE is influenced by the state probabilities in the Markov model, the inverter size, and the average power generation time of the modules throughout the year, as discussed earlier. Figure 7(b) shows the relationship between the ELCOE and the number of inverters, considering the prices in 2022 and an average power generation time of $h = 2.4$ [hours/day]. Two interesting points are highlighted: (1) a local optimal solution is observed at $n_i = 3$, while a global optimal solution is found at $n_i = 5$ within the search domain. This distinction is attributed to the fact that the ELCOE is influenced not only by probabilities, as observed in the NSEE, but also by the costs of inverters and their

associated maintenance and repair expenses. In Figure 7(c), the ELCOE is plotted as a function of the number of inverters, considering the prices in 2012 and an average power generation time of $h = 2.4$ [hours/day]. The results exhibit a similar behaviour.

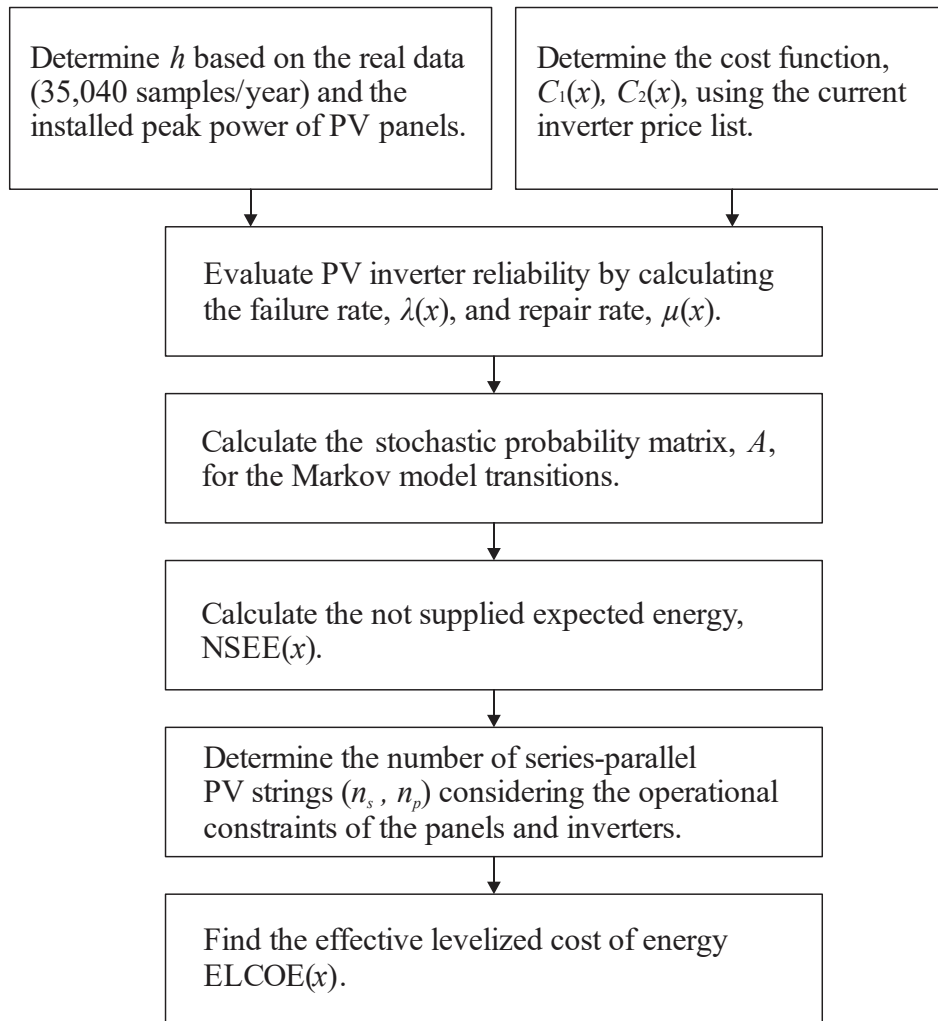


Figure 6: Optimal design flowchart.

Table 1: Summary of results.

n_i	x [kW]	NSEE [kWh/1-day]	$h = 2.4$ [hours/day]		$h = 6$ [hours/day]	
			ELCOE 2012 [\$/kWh]	ELCOE 2022 [\$/kWh]	ELCOE 2012 [\$/kWh]	ELCOE 2022 [\$/kWh]
1	100	7363.60	16.35	7.83	6.54	3.13
2	50	727.67	2.21	0.94	0.88	0.37
3	30	516.48	1.85	0.85	0.74	0.34
4	25	582.53	1.93	0.92	0.77	0.47
5	20	38.99	0.91	0.39	0.36	0.15
6	15	30.25	0.91	0.41	0.36	0.16

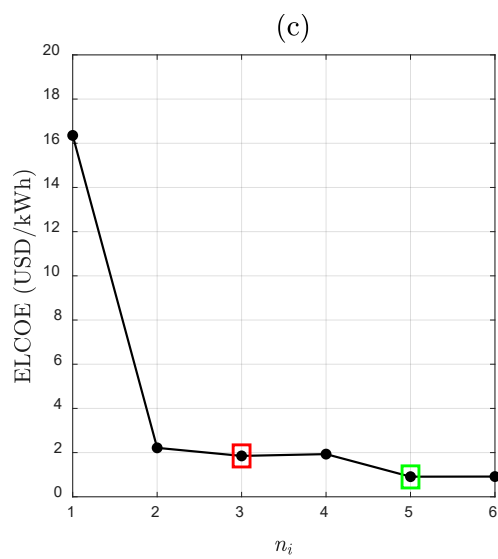
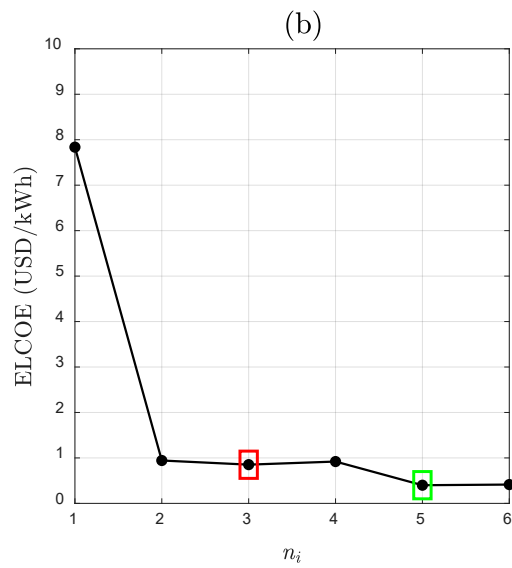
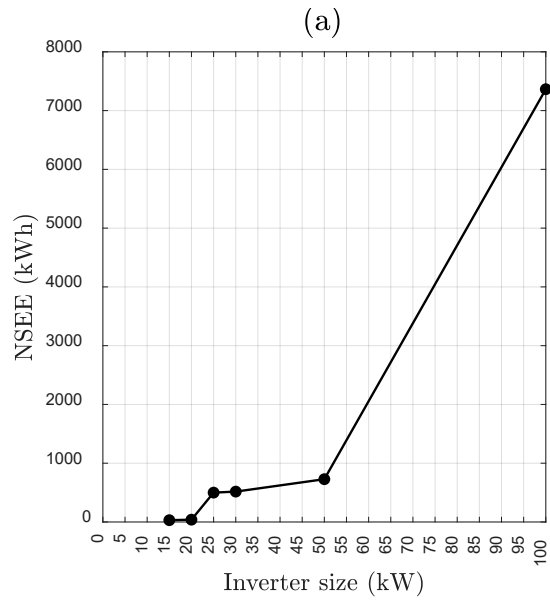


Figure 7: (a) NSEE as a function of inverter size, (b) ELCOE in 2022, (c) ELCOE in 2012.

5. CONCLUSIONS

In conclusion, this paper addresses the challenge of energy generation through renewable sources, specifically focusing on PV stations. The research presents a methodology that calculates key variables crucial to PV station design, building upon previous studies and incorporating real-world data from PV station components. The investigation primarily centres around the behaviour of PV inverters, which are vital components of PV stations. Using the Markov model and proposing a new price model, the study analyses the long-term performance of PV stations, considering current costs associated with PV inverters.

A notable contribution of this research is the comparative analysis of various PV station configurations, accounting for geographical variations and changes in PV inverter costs. The consistent results demonstrate the superiority of the proposed method, leading to improved outcomes and convergence towards optimal solutions in terms of energy levelized cost of electricity for PV stations up to 100 kW. Overall, this study provides valuable insights and practical guidance for the design and optimization of PV stations, contributing to the advancement of renewable energy generation.

REFERENCES

- [1] Fraunhofer ISE, ‘Current and Future Cost of Photovoltaics: Long-term Scenarios for Market Development, System Prices and LCOE of Utility-Scale PV Systems’, 2015. https://www.ise.fraunhofer.de/content/dam/ise/de/documents/publications/studies/AgoraEnergiewende_Current_and_Future_Cost_of_PV_Feb2015_web.pdf (accessed Jun. 23, 2023).
- [2] M. Roser, ‘The world’s energy problem’, 2020. <https://ourworldindata.org/worlds-energy-problem> (accessed Jun. 23, 2023).
- [3] M. Roser, ‘Why did renewables become so cheap so fast?’, 2023. <https://ourworldindata.org/cheap-renewables-growth> (accessed Jun. 23, 2023).
- [4] C. Le Quéré and P. Friedlingstein, ‘Global Carbon Budget 2021’, 2021. https://www.globalcarbonproject.org/global/images/carbonbudget/Infographic_Emissions2021.pdf (accessed Jun. 23, 2023).
- [5] D. S. Philipps, F. Ise, W. Warmuth, and P. P. GmbH, ‘Photovoltaics Report’, 2023. <file:///C:/Users/aoga3005/Downloads/Photovoltaics-Report.pdf> (accessed Jun. 23, 2023).
- [6] ‘Solar Market Insight Report 2022 Q3’, 2023. <https://www.seia.org/research-resources/solar-market-insight-report-2022-q3> (accessed Jun. 23, 2023).
- [7] P. Gevorkian, *Large-scale solar power system design: an engineering guide for grid-connected solar power generation*. McGraw-Hill Education, 2011.
- [8] T. Kerekes, E. Koutroulis, D. Séra, R. Teodorescu, and M. Katsanevakis, ‘An Optimization Method for Designing Large PV Plants’, *IEEE J. Photovolt.*, vol. 3, no. 2, pp. 814–822, Apr. 2013, doi: 10.1109/JPHOTOV.2012.2230684.
- [9] Z. Moradi-Shahrbabak, A. Tabesh, and G. R. Yousefi, ‘Economical Design of Utility-Scale Photovoltaic Power Plants With Optimum Availability’, *IEEE Trans. Ind. Electron.*, vol. 61, no. 7, pp. 3399–3406, Jul. 2014, doi: 10.1109/TIE.2013.2278525.
- [10] M. Theristis and I. A. Papazoglou, ‘Markovian Reliability Analysis of Standalone Photovoltaic Systems Incorporating Repairs’, *IEEE J. Photovolt.*, vol. 4, no. 1, pp. 414–422, Jan. 2014, doi: 10.1109/JPHOTOV.2013.2284852.
- [11] R. Billinton and R. N. Allan, *Reliability Evaluation of Engineering Systems*. Boston, MA: Springer US, 1992. doi: 10.1007/978-1-4899-0685-4.

- [12] HUAWEI, ‘SUN2000-(70KTL,75KTL)-C1: User Manual’, Mar. 13, 2023. file:///C:/Users/aoga3005/Downloads/SUN2000-(70KTL,75KTL)-C1%20User%20Manual.pdf (accessed Jun. 23, 2023).
- [13] D. Moser, ‘Technical Risks in PV Projects, Report on Technical Risks in PV Project Development and PV Plant Operation’, 2017. https://www.tuv.com/content-media-files/master-content/services/products/p06-solar/solar-downloadpage/solar-bankability_d1.1_d2.1_technical-risks-in-pv-projects.pdf (accessed Jun. 23, 2023).
- [14] ‘SUN2000-(100KTL-M1): User Manual’, Mar. 30, 2020. <https://www.ske-solar.com/wp-content/uploads/2020/08/Handbuch-Huawei-SUN2000-100KTL-M1.pdf> (accessed Jun. 23, 2023).
- [15] M. E. Alkal, ‘Entwurf eines Modells für die Vorhersage der eingespeisten, erneuerbaren Energie mittels Künstlicher Neuronaler Netze (Draft of a model for the prediction of the renewable energy fed into the grid by means of artificial neural networks)’, Studienarbeit, Technische Universität Ilmenau, Ilmenau, 2010.
- [16] A. Gabash, M. E. Alkal, and P. Li, ‘Impact of allowed reverse active power flow on planning PVs and BSSs in distribution networks considering demand and EVs growth’, *Power Energy Stud. Summit PESS 2013 IEEE Stud. Branch Bielef.*, pp. 11–16, 2013.
- [17] M. Alramlawi, A. Gabash, E. Mohagheghi, and P. Li, ‘Optimal operation of hybrid PV-battery system considering grid scheduled blackouts and battery lifetime’, *Sol. Energy*, vol. 161, pp. 125–137, Feb. 2018, doi: 10.1016/j.solener.2017.12.022.

CONTACTS

M.Sc. Marcio B. Salazar Márquez	email: marcio-boris.salazar-marquez@tu-ilmenau.de
Dr.-Ing. Aouss Gabash	email: aouss.gabash@tu-ilmenau.de
Prof. Dr. Yuri A.W. Shardt	email: yuri.shardt@tu-ilmenau.de
Prof. Julio C. Tafur	email: jtafur@pucp.edu.pe